

1 **Brief Communication: Antarctic sea ice loss brings observed trends** 2 **into agreement with climate models**

3 Caroline R. Holmes¹, Thomas J. Bracegirdle¹, Paul R. Holland¹, Julienne Stroeve^{2,3,4}, Jeremy Wilkinson¹

4 ¹British Antarctic Survey, Cambridge, CB3 0ET, UK

5 ²National Snow and Ice Data Center, Cooperative Institute for Research in Environmental Sciences, University of Colorado,
6 Boulder, Colorado, USA

7 ³Centre for Earth Observation Science, University of Manitoba, Winnipeg, Manitoba, Canada

8 ⁴Earth Sciences, University College London, London, UK

9 *Correspondence to:* Caroline R. Holmes (calmes@bas.ac.uk)

10 **Abstract.** Most climate models do not reproduce the 1979-2014 increase in Antarctic sea ice cover. This was a contributing
11 factor in successive Intergovernmental Panel on Climate Change (IPCC) reports allocating low confidence to model
12 projections of sea ice over the 21st century. We show that recent rapid declines bring observed sea ice area trends into line
13 with the models. This implies that projections of substantial future Antarctic sea ice loss may be more reliable than previously
14 thought, with wide-ranging implications for the evolution of the Southern Hemisphere climate.

15 **1 Introduction**

16 The early years of the twenty-first century revealed a puzzling conundrum in Antarctic sea ice (Turner and Comiso, 2017;
17 National Academies of Sciences and Medicine, 2017). Observations of Antarctic sea ice extent (SIE) showed a small increase
18 during the satellite era (which began in late 1978), with annual mean values reaching a maximum in 2014, but most climate
19 models simulated SIE declines over the same period. Various studies examined possible reasons for this discrepancy (Turner
20 and Comiso, 2017). Specifically, the community discussed whether it could be explained by internal variability masking the
21 anthropogenic forced signal in observations (Gagné et al., 2015; Rosenblum and Eisenman, 2017; Roach et al., 2020) and the
22 extent to which it revealed model deficiencies in sea ice processes (Fox-Kemper, 2021). Some studies found that the observed
23 pan-Antarctic trends lay within the distribution of modelled trends (Polvani and Smith, 2013; Zunz et al., 2013) and that only
24 regional trends could robustly be deemed inaccurate in the models (Hobbs et al., 2015). However, these studies considered
25 trends to 2005 only, and over this 27-year period the role of internal variability is larger than with more recent end dates.
26 Others suggested that trends in sea ice, particularly SIE, may not be a robust metric of model performance, particularly when
27 the observational time series is too short to separate internal variability from anthropogenic forcing (Notz, 2014). Even so, the
28 poorly understood discrepancy between models and observations has been a contributing factor in a widespread lack of
29 confidence in projections of 21st century Antarctic sea ice decline, and consequently in many aspects of projected climate

30 change around Antarctica, which are underpinned by projections of substantial sea ice decline (Bracegirdle et al., 2015;
31 Bracegirdle et al., 2018).

32
33 Recently, Antarctic sea ice has exhibited a starkly different pattern of behaviour. Following the pre-2015 era of slightly
34 increasing ice extent, rapid ice loss beginning in early 2015 culminated in a dramatic drop in spring 2016-17 (Turner et al.,
35 2017). This led to several years of record low SIE, which has been framed as a ‘new sea ice state’ (Purich and Doddridge,
36 2023; Hobbs et al, 2024). This situation shows no sign of abating, with further declines since 2021 leading to monthly-mean
37 SIE records being broken in eight months of 2023 (Fetterer, 2017; Siegert et al., 2023). The initial decline showed strong
38 linkages to patterns of intrinsic atmospheric variability (Turner et al., 2017; Schlosser et al., 2018; Zhang et al., 2022) which
39 have high internal variability on short (sub-annual) timescales. However, growing evidence of the contribution of warming in
40 the subsurface ocean (Zhang et al., 2022; Purich and Doddridge, 2023), and the magnitude and spatial homogeneity of the sea
41 ice reductions since 2016/17, point to more sustained declines.

42
43 In light of this sea ice loss, we re-consider whether the distribution of trends simulated by the current generation of climate
44 models, from the Coupled Model Intercomparison Project Phase 6 (CMIP6; Eyring et al., 2016) dataset, allows for a trend of
45 the observed magnitude and thus whether observed trends are consistent with the multi-model ensemble. Key previous studies
46 have considered trends to 2005 (Hobbs et al., 2015; Polvani and Smith, 2013; Zunz et al., 2013) or 2013 (Rosenblum and
47 Eisenman, 2017) based on CMIP5 models and to 2018 based on CMIP6 (Roach et al., 2020). We might expect the situation to
48 have changed, for two reasons. First, being able to assess trends in longer timeseries (due to the longer observational record)
49 potentially reduces the impact of short-term internal variability on trend calculations (Notz, 2014). Second, and more
50 specifically, these data now include the recent years of observed rapid decline of sea ice, decreasing long-term trends. Therefore
51 we perform an analysis of all trends with end dates between 2005 and 2023, to place our results in the context of previous
52 studies and show how the results change over time due to these two factors, while using a consistent set of CMIP6 model data
53 (such that the changes are not attributable to changes in model components or resolution).

54 **2. Data and Methods**

55 **2.1 Sea Ice Metric**

56 Sea ice cover is calculated as either sea ice extent, SIE (the total area of all gridboxes where sea ice concentration SIC exceeds
57 a 15% threshold), or sea ice area, SIA (the sum of gridbox areas multiplied by gridbox SIC). SIA has larger observational
58 uncertainties, as it is more sensitive to differences in SIC. However, SIE is a non-linear measure and so can give misleading
59 results when comparing models and observations or when calculating trends (Notz, 2014). Therefore, in contrast to some
60 previous assessments, but following community precedent (Roach et al., 2020), we assess SIA. SIA and SIE have similar
61 trends (Fig. A1).

62 **2.2 Model Data**

63 We use data from 39 CMIP6 models, from multiple modelling centres. Across the ensemble, there are multiple different model
64 components and resolutions of each component. Monthly SIA is obtained from the University of Hamburg (UHH) CMIP6 Sea
65 Ice Area directory (<https://www.cen.uni-hamburg.de/en/icdc/data/cryosphere/cmip6-sea-ice-area.html>, accessed 2023-08-17)
66 and aggregated into weighted annual means. This is supplemented by SIA for the two NorESM models, which are not available
67 in the UHH dataset due to a bug in an earlier version of NorESM released SIA data. We merge historical simulations ending
68 in December 2014 with the ssp585 forcing scenario run for 2015 to 2023. ssp585 indicates a global average radiative forcing
69 of 8.5 W m^{-2} by 2100 (O'Neill et al., 2016). This is a high-emissions forcing scenario; however, emissions scenarios have little
70 bearing on results for the time period considered here. The resulting historical-ssp585 merger constitutes 188 ensemble
71 members from 39 models (Table A1), each contributing between 1 and 57 members of an initial condition ensemble.

72
73 By using a large number of ensemble members of the historical multi-model ensemble, we sample internal variability under
74 historical anthropogenic forcing. However, since only four models contain more than six members, we use a maximum of six
75 members from each model to avoid weighting the results too heavily towards models with large ensembles. Thus the final
76 ensemble analyzed has 98 members (Fig. B1) from 39 models (Table B1). The sensitivity of our results to this treatment of
77 model ensembles and to the emission scenario is discussed in Appendix C.

78
79 Since many models have drifts in their pre-industrial runs, we calculated linear trends over the full pre-industrial period
80 available (in the range 150 to 500 years across the 32 models with data available in the UHH dataset; Table B1), henceforward
81 referred to as 'drift'. In all cases, drifts are an order of magnitude smaller than the trends for years 1979-2023, and there is no
82 significant inter-model relationship between the drift in a model's pre-industrial simulation and the ensemble mean of linear
83 trends in that model ($p=0.48$). This implies drifts are negligible in the context of historical trends, consistent with results for
84 CMIP5 (Gupta et al., 2013), and so they are not considered further.

85 **2.3 Observational Data**

86 For an estimate of observed sea ice cover, NSIDC Sea Ice Index v3.0 SIA (Fetterer, 2017) is used, available from January
87 1979-September 2023. We investigate the role of observational uncertainty by also using other observational estimates for
88 1979-2019 from the UHH SIA dataset (Dörr, 2021). Data for missing months (December 1987-January 1988 for the Sea Ice
89 Index v3.0) are infilled by interpolating between the same month in the previous and following year (Rosenblum and Eisenman,
90 2017).

91 **2.4 Trend evaluation methodology**

92 Our evaluation methodology is an extension of that previously used for CMIP5 (Rosenblum and Eisenman, 2017). Linear
93 trends are calculated for all periods of at least 35 years overlapping with the satellite record (January 1979-September 2023)
94 using the OLS method of the Python package statsmodels.api. For comparison with the earlier studies mentioned in the
95 Introduction, we additionally calculate trends for periods 1979–y2 where y2 is between 2005 and 2012. We calculate the mean
96 and standard deviation of the trends from the model ensemble and use these to fit a Gaussian distribution, with cumulative
97 distribution function $F(X)$, to the distribution of modelled these trends. To estimate the probability that a trend at least as large
98 as observed would occur in the climate model population, we calculate the p-value for a one-tailed test as $1-F(x)$, where x is
99 the observed trend. The extent to which a linear trend is an appropriate description of the time evolution of SIA is considered
100 in the Discussion below.

101 **3 Results**

102 **3.1 Trend evaluation**

103 The recent decade of data has reduced the significant positive trend (Parkinson, 2019) in observed annual-mean and monthly
104 SIA, which peaked in the period ending 2015, to near-zero (Fig. 1a)-c), red lines; Fig. C1a, A1). For some months and in the
105 annual mean, the trend since 1979 is now weakly negative, and trends are statistically insignificant in all months (Fig. A1).
106 Meanwhile, adding the extra years of data hardly changed the multi-model mean trend at all (Fig. 1a)-c), blue lines). The mean
107 trend remains strongly negative, although a few simulations have weakly positive trends. The simulated trends are less
108 influenced by internal climate variability as more years are added, and therefore the standard deviation of the modelled trends
109 for a fixed start year of 1979 decreases over time (Fig. C1c).

110
111 In light of these findings, we test the null hypothesis that observed sea ice trends are consistent with trends simulated across
112 the CMIP6 multi-model ensemble, and consider how additional years of data affect the outcome of this test. We consider
113 trends calculated with both a fixed start date (1979) and fixed duration (35 years) to aid our interpretation. Until 2010 inclusive,
114 the probability of a CMIP6 model trend matching or exceeding the observed trend exceeds 0.05, so we would accept the null
115 hypothesis that modelled and observed trends are consistent (as concluded in Zunz et al., 2013; Hobbs et al., 2015; Polvani
116 and Smith, 2013)). However, in the period 2005 through 2015, the multi-model mean trend and observed trend diverge while
117 the modelled trend distribution narrows (Fig. C1), reducing the likelihood that the observed trend falls within the modelled
118 distribution. As a result, between 2011 and 2018, the probability of a CMIP6 model trend matching or exceeding the observed
119 trend is very low ($p < 0.05$; Fig. 1d), so the null hypothesis is rejected and the model trends may be deemed inconsistent with
120 observations. This test provides a clear result; the short time period of under forty years should allow for a generous range of
121 modelled trends due to internal variability, but this range still fails to accommodate the observations.

122

123 From 2015, the probability of CMIP6 trends matching or exceeding the observed trend starts to increase, as the ice loss brings
 124 observations into line with the models (Fig. 1d). However, if trends are calculated with a fixed 1979 start date, progressively
 125 lengthening the trend under consideration decreases the modelled trend standard deviation while hardly affecting the model
 126 mean trend (Fig. C1). This makes it less likely that the observed trends will fall within the distribution of modelled trends.

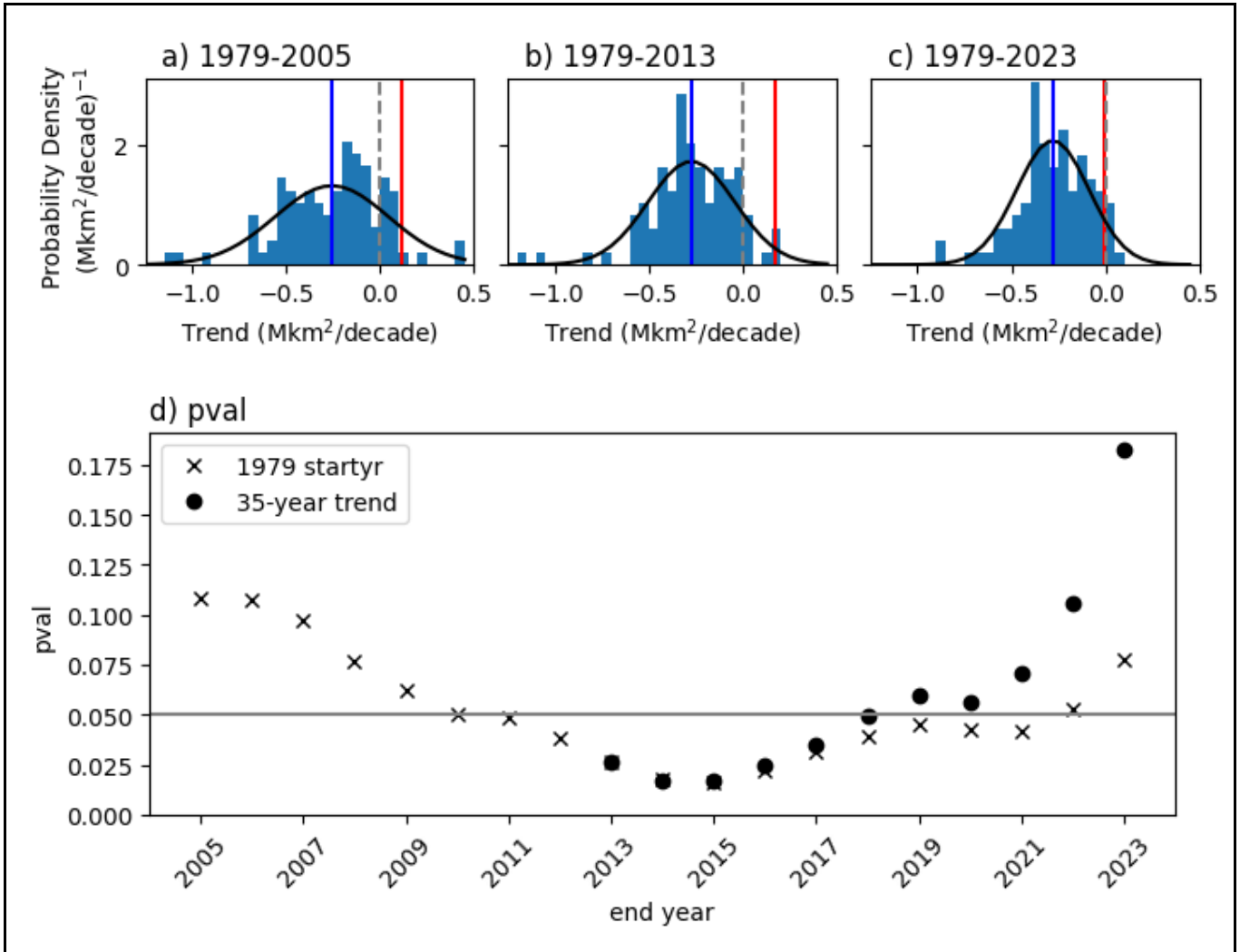


Figure 1 (a-c) Linear trends in annual mean SIA in satellite observations (red) and CMIP6 models (blue histogram) and Gaussian fit to CMIP6 distribution (black) for the periods (a) 1979-2005, (b) 1979-2013 and (c) 1979-2023. The dashed vertical line indicates zero trend and the blue line indicates the multi-model mean. (d) the probability of observing a trend at least as large as observed (a one-tailed test) under the null hypothesis that observations are taken from the same population as the CMIP6 multi-model ensemble, for varying end dates and either a fixed start date of 1979 as in panels a) and b) (crosses) or fixed trend length of 35 years (dots).

127 Only in 2022 does the recent rapid decline in observations counteract this effect and finally bring observed trends into line
 128 with the models (null hypothesis not rejected at $p=0.05$; Fig. 1d). In contrast, for ‘fixed duration’ trends, the standard deviation

129 of modelled trends remains large, while the observed trend more rapidly declines and becomes negative due to the neglect of
130 early low SIA years (Gagné et al., 2015; Schroeter et al., 2023) in addition to the inclusion of the recent low SIA years.
131 Therefore, the null hypothesis is no longer rejected at $p=0.05$ as early as 2019 under this measure.

132

133 **3.2 Relationship of trends with mean state**

134 It is known that, seasonally and especially in summer, there is a relationship between sea ice area climatology and future trends,
135 which is to be expected as, for example, very low sea ice constrains trends (Holmes et al, 2022). Therefore, we investigated
136 the relevance of this for our trend assessment. The relationship between both summer and annual mean climatology and the
137 annual mean trends is highly statistically significant, but has a very weak slope (Fig C2a,b). Since there are two models (from
138 the MIROC family) which are clear outliers, having far too little sea ice in the annual mean (Fig C2b; Shu et al, 2020), we test
139 the sensitivity to removing these models. This does not change our conclusion that trends are consistent for an end date of
140 2023 (Fig. C2c). Therefore, while there is some evidence that the models with trends closest to observations tend to be biased
141 low (Fig. C2a,b), this does not appear to dominate our conclusion that observed and modelled trends are now consistent.

142

143 **4 Discussion and Conclusions**

144 Our results show that the consistency between observed and modelled trends changes over time. Firstly, for early end dates
145 (prior to 2011) there is no evidence of inconsistency between observed and modelled trends, as noted by earlier studies (Hobbs
146 et al., 2015; Zunz et al., 2013; Polvani and Smith, 2013). Secondly, there is a mismatch between observed and modelled trends
147 for the period up to around 2018, as discussed in the Introduction, suggesting that modelled anthropogenic trends are too strong
148 relative to modelled variability during that period. Finally, our study shows the novel result that the persistent low Antarctic
149 SIA of 2022 and 2023 brings observed trends back into line with the ensemble of modelled trends, permitting the interpretation
150 that modelled forced trends and variability are realistic on 45-year timescales (the full length of the modern satellite record).
151 This is an important conclusion, since these longer timescales are of greatest relevance to centennial projections of climate
152 change, and to the attribution of anthropogenically forced change. Moreover, even trends on the shorter 35-year timescale fall
153 within the model ensemble for the five most recent 35-year periods (Fig. 1d).

154 Focussing on trends with a fixed start date, the changing assessment of skill with increasing years of data could be explained
155 in several ways. Conceptually, for any time period there is a distribution of model trends and also a distribution of possible
156 real trends that could have occurred (depending upon the evolution of internal climate variability). The observed trend is a
157 single realisation of the distribution of possible real trends. The observed trends with end dates between 2011 and 2021 were
158 outside the model trend distribution. Now, the latest observed trends fall within with the distribution of modelled trends, as do
159 observed trends for periods ending before 2011. In other words, the observed trends over the middle period lay in the region

160 where the modelled and real trend distributions did not overlap, and observed trends in the earlier and most recent periods lie
161 in the region where they do overlap.

162

163 The modelled and real trend distributions will differ in their spread if the models have inaccurate variability, and in their mean
164 if the models have an inaccurate anthropogenic forced trend. Therefore, inaccurate variability, particularly on multidecadal
165 timescales, could explain the changing assessment of skill. Indeed, modelled variability exceeds observed variability and varies
166 greatly between models (Zunz et al., 2013, Roach et al., 2020, Diamond et al., 2024), with some models containing large
167 centennial variability (Zhang et al., 2019). Alternatively, it could be that the modelled anthropogenic trends are too strong
168 (Schneider and Deser, 2018), or emerge too early. For example, this is consistent with the hypothesis that models under-
169 estimate the timescale or magnitude of the cooling phase of the ‘two-timescale’ response to stratospheric ozone forcing,
170 whereby increasing westerlies cause a cooling (sea ice increase) on ‘short’ timescales and warming (decline) on ‘long’
171 timescales (Ferreira et al., 2015; Kostov et al., 2017). However, other evidence from models suggests this mechanism is
172 unlikely to be a primary driver of the model-observation mismatch (Seviour et al., 2019). The latest observed ice decline may
173 be finally revealing the influence of anthropogenic forcing, bringing the observations closer to the models, which have long
174 predicted a decline.

175

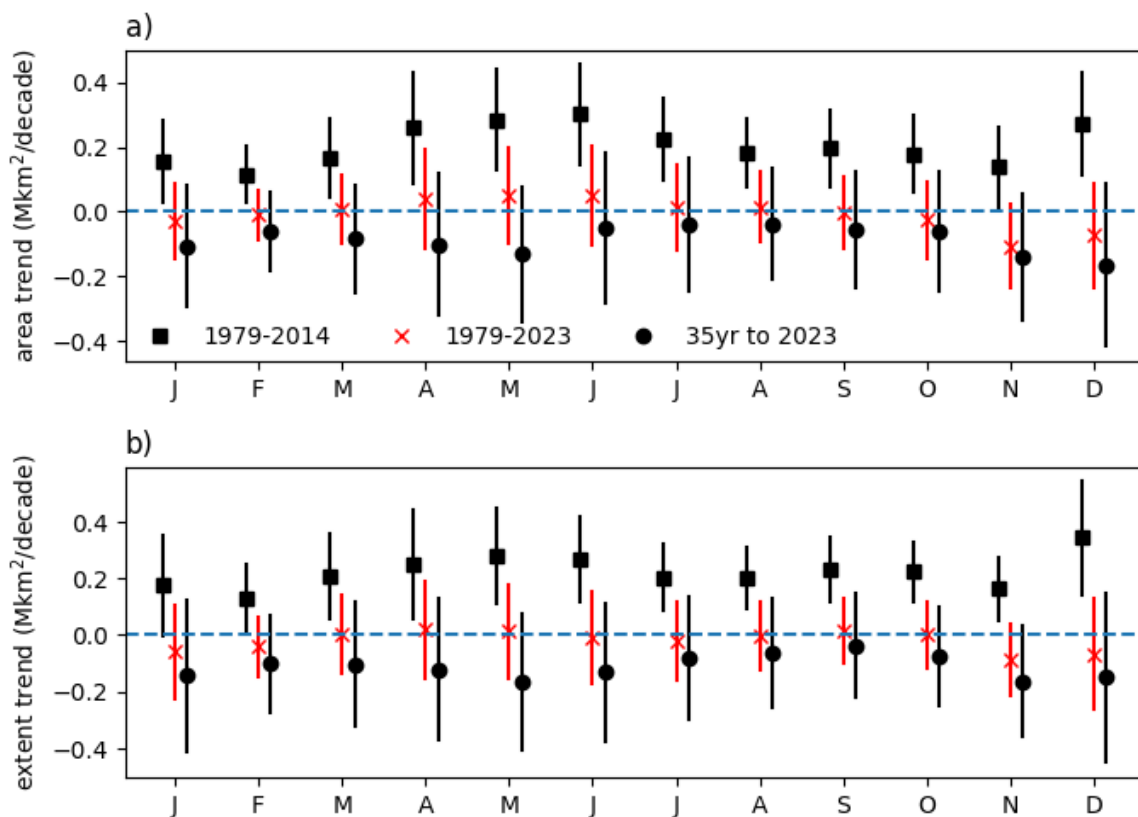
176 The importance of our results is in showing that we can no longer rule out climate model simulations of Antarctic sea ice based
177 on linear trends alone. There are of course many further measures by which modelled sea ice may be assessed, including
178 seasonal and interannual variability (Zunz et al., 2013), spatial patterns (Hobbs et al., 2015), physical processes (Holmes et al.,
179 2019), and relationships between trends and other variables (e.g. global warming; Rosenblum and Eisenman, 2017 or mean
180 state, as discussed above). Moreover, linear trends are a limited parametric assessment of a timeseries and one could argue that
181 the observed time series appears to display more complexity than a linear trend with noise imposed (Fig B1). However,
182 complex behaviours, revealing the interplay of trends and variability including on long timescales, are also apparent in
183 individual model ensemble members (Fig B1). Therefore, our argument is simply that being able to simulate linear trends is a
184 fundamental test, and models no longer fail this fundamental test, at least over the 45-year modern satellite era. Future studies
185 can therefore move on to more detailed model assessments, including representation of the recent rapid decline itself (Diamond
186 et al., 2024). The rapid decline is as yet short-lived, so an improved understanding of multi-decadal sea ice variability and its
187 representation in climate models is critical for further interpreting these results. Further, processes lacking from models, such
188 as increasing freshwater input from accelerating ice sheet melt (Swart et al., 2023), may provide further complications in the
189 relative evolution of modelled and observed sea ice over the 21st century.

190

191 Our results have broad ramifications for future assessments of CMIP6 outputs. First, revising our confidence in the climate
192 models has consequences for the attribution of historical climate changes. Secondly, we should now have some level of greater
193 confidence in the strong projected declines in Antarctic sea ice under anthropogenic forcing (Roach et al., 2020), whereby ice

194 becomes near-absent in summer (Holmes et al., 2022). This in turn will influence our understanding of the future evolution of
195 all aspects of the Southern Hemisphere climate - including Southern Ocean heat and carbon uptake, circumpolar winds
196 (Bracegirdle et al., 2018), and melting of the Antarctic Ice Sheet – and of marine ecosystem function; all of which underpins
197 decisions about the mitigation of future greenhouse gas emissions and about ecosystem management.

198 **Appendix A: Monthly trends**



200
201 **Figure A1: Observed sea ice trends in individual months for (squares) 1979-2014, (crosses) full 45-year trend 1979-**
202 **2023, and (circles) 35-year trend to 2023. 1979-2023 trends are highlighted in shades of red as this period is the focus**
203 **of the paper. a) Sea Ice Area, b) Sea Ice Extent. 5th-95th percentile uncertainties are indicated by vertical lines. Data**
204 **are from the Sea Ice Index (see Methods).**

205

Appendix B: CMIP6 models

Model	Mean Trend			Climatology		Trend piControl	n members used (available)
	1979-2013	1979-2023	1989-2023	February 1979-2023	Annual 1979-2023		
ACCESS_CM2	-0.049	-0.173	-0.265	0.532	7.435	-0.021	1
ACCESS_ESM1	-0.151	-0.099	-0.104	2.120	8.238	N/A	3
AWICM1	-0.405	-0.473	-0.420	1.171	9.802	0.004	1
BCC_CSM2	0.194	-0.443	-0.803	0.294	6.644	-0.027	1
CAMS_CSM1	-0.067	-0.096	-0.230	0.012	5.846	-0.023	2
CESM2	-0.369	-0.382	-0.388	1.602	8.960	-0.007	3
CESM2_WACCM	-0.474	-0.447	-0.446	1.760	9.181	-0.012	3
CIESM	-0.251	-0.261	-0.261	0.079	5.487	-0.019	1
CMCC_CM2_SR5	-0.356	-0.330	-0.328	0.679	7.568	-0.040	1
CMCC_ESM2	-0.297	-0.247	-0.254	0.719	7.699	-0.045	1
CNRM_CM6	-0.362	-0.379	-0.376	0.940	9.192	-0.018	6
CNRM_CM6_1_HR	-0.443	-0.583	-0.950	0.499	8.065	-0.065	1
CanESM5	-0.386	-0.356	-0.373	4.014	11.841	0.005	6 (19)
E3SM_1_1	-0.323	-0.360	-0.422	1.320	9.166	0.003	1
ECEarth3	-0.267	-0.222	-0.236	0.263	4.654	-0.009	6 (57)
ECEarth3_CC	-0.231	-0.126	-0.147	0.056	3.187	-0.013	1
ECEarth3_Veg	-0.149	-0.196	-0.276	0.298	4.816	-0.008	5
ECEarth3_Veg_LR	-0.325	-0.280	-0.293	0.182	4.819	-0.005	1
FGOALS_f3L	-0.122	-0.159	-0.109	0.277	6.360	N/A	1
FGOALS_g3	-0.279	-0.226	-0.135	2.214	10.813	0.000	4
FIO_ESM	-0.316	-0.342	-0.339	2.035	9.448	-0.001	3
GFDL_CM4	-0.223	-0.193	-0.159	0.529	9.791	-0.019	1
GFDL_ESM4	-0.039	-0.111	-0.075	0.641	8.455	-0.019	1
GISS_E2_1_G	-0.135	0.008	0.062	0.731	8.049	N/A	1
HadGEM3_GC31_LL	-0.514	-0.607	-0.674	1.957	8.692	N/A	3
HadGEM3_GC31_MM	-0.312	-0.313	-0.362	1.482	6.144	-0.047	4
INM_CM4_8	-0.193	-0.210	-0.228	0.242	4.386	-0.012	1
INM_CM5_0	-0.238	-0.232	-0.200	0.904	6.231	0.021	1
IPSL_CM6A_LR	-0.363	-0.384	-0.414	1.616	10.606	0.006	6
KIOST_ESM	-0.259	-0.215	-0.156	0.725	6.252	N/A	1
MIROC6	-0.014	-0.015	-0.006	0.017	1.505	-0.001	3
MIROC_ES2L	-0.072	-0.084	-0.108	0.019	1.398	0.002	6 (8)

MPI_ESM1_2_HR	-0.277	-0.274	-0.356	0.298	5.833	-0.004	2
MPI_ESM1_2_LR	-0.108	-0.078	0.019	0.259	4.325	0.000	6 (30)
MRI_ESM2	-0.325	-0.377	-0.436	2.537	11.964	-0.009	1
NESM3	-0.202	-0.283	-0.374	0.485	7.746	-0.010	2
NorESM2_LM	-0.096	-0.082	-0.102	1.385	6.238	N/A	1
NorESM2_MM	-0.014	-0.077	-0.041	1.402	6.543	N/A	1
UKESM1_0_LL	-0.721	-0.666	-0.652	2.947	9.954	0.005	5

207

208

209

210

211

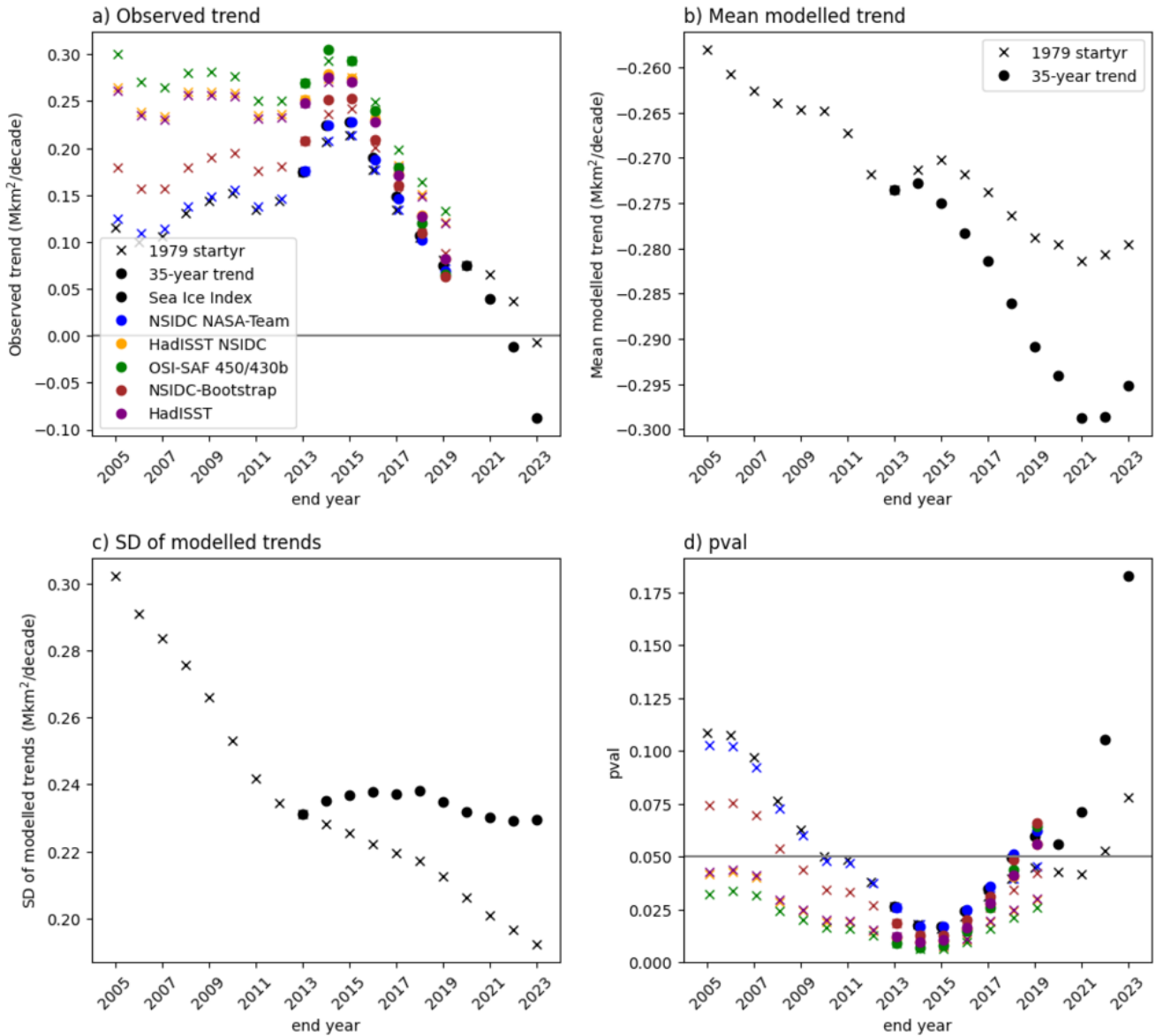
212

Table B1: The models available for the study and summary values: the number of ensemble members number used (and the number available where this differs); the ensemble mean trend (Mkm²/decade) and the climatology (Mkm²) across the ensemble members used only for the period specified; and the trend in the pre-industrial simulation (Mkm²/decade) . NorESM values were calculated by the authors from SIC data; all other values were obtained from the CMIP6 SIA Directory made available by the University of Hamburg and methods are fully detailed there.



Figure B1: 1979-2023 annual mean sea ice area in observations (Sea Ice Index v3, top left) and in all CMIP6 model ensemble members considered in the analysis. Panels are sorted by their linear trend over 1979-2023. Linear trends are shown and indicated in red (statistically significant at $p < 0.05$) or grey (statistically insignificant). Each panel includes annotation showing the simulation's 1979-2023 climatology and trend. Y-axis shows SIA anomaly from 1979-2023 climatology (Mkm^2).

Appendix C: Sensitivity Tests



216

217 **Figure C1: Contributions to the p-value shown in Figure 1d). a) observed trend; Sea Ice Index in black as in main text,**
 218 **other datasets as indicated. b) mean of modelled trends, c) standard deviation of modelled trends, d) p-value (as main**
 219 **text Figure 1d but with alternative observational estimates (Dörr, 2021)).**

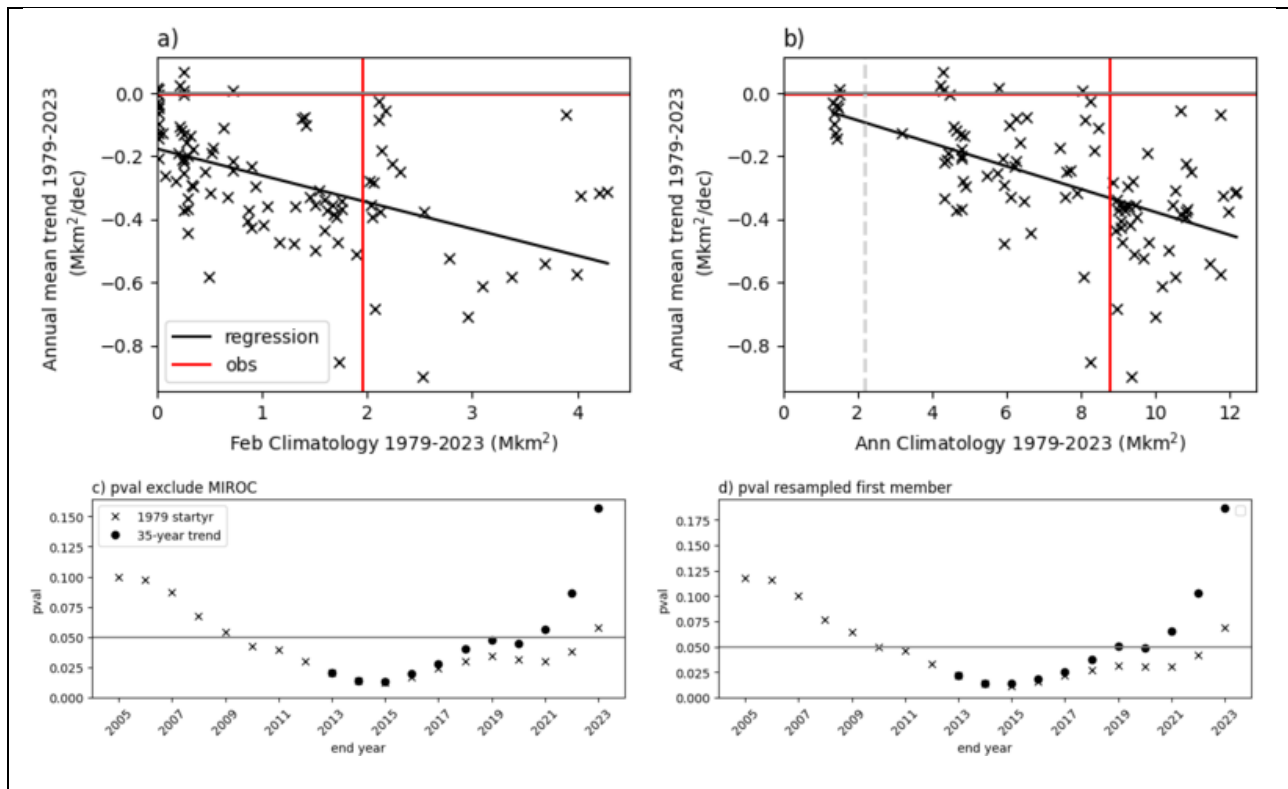


Figure C2: The role of ice-free conditions in explaining model spread, and result sensitivity to ensemble treatment. a) Scatter plot of summer (February) sea ice climatology for 1979-2023 against the annual-mean trend over 1979-2023. Maximum 6 ensemble members per model shown. b) as a) but for annual mean climatology against trend, with cutoff threshold (observed climatology/4) to exclude MIROC models indicated in grey dashed line. c) As figure 1d) but excluding MIROC models. d) As figure 1d) but using 1 random ensemble member from each model, resampled 10000 times; mean of p-values.

220 Sensitivity to Observational Dataset

221 Observational uncertainty in SIA is particularly high prior to winter 1987 (not shown) due to missing SIC data. Trends in the
 222 other datasets, in particular OSI-SAF (Figure C1, green), are in general more strongly positive than those in the Sea Ice Index
 223 (Figure C1a). Therefore, for the ‘1979 start date’ trends, these might exhibit consistency with model-simulated trends at later
 224 end dates than 2022 (Figure C1d, crosses); note that all datasets already display consistency for the 35-year trends ending in
 225 2019 onwards (Figure C1d, dots).

226 Sensitivity to treatment of CMIP6 models

227 We also tested the sensitivity of our conclusions to our treatment of CMIP6 models. First, we tested the sensitivity to treatment
 228 of individual model ensembles. As stated in the main text, the choice of using a maximum of six ensemble members per model
 229 was to sample internal variability adequately without weighting towards models with large ensembles. By including all
 230 ensemble members (instead of a maximum of six per model), we largely add simulations from models with weak negative

231 average trends (Table B1) and so increase consistency with observations (not shown). However, the evolution with end year
232 of the model-observation comparison (Fig. 1d) and the broad timings of threshold crossings are unchanged. On the other hand,
233 since curtailment to a maximum six members per model still constitutes uneven sampling across models which have different
234 internal variabilities, we also verified that when using one ensemble member per model, results remain on average the same
235 for 2023 end dates (Fig. C2d).

236
237 Second, we tested sensitivity to using the weaker forcing scenario ssp245 instead of ssp585 for the extension of modelled
238 trends after 2014. The effect of forcing scenario is small early in the 21st century (Hawkins and Sutton, 2012), so that any
239 difference arising is due to internal variability or structural differences between the models with simulations available. For the
240 overlapping subset of 147 model-realisation combinations, ssp245 has marginally stronger trends and so is slightly less
241 consistent with observations. In contrast, using the full ssp245 ensemble (with all available members) means including a larger
242 ensemble of MIROC6 than in the overlapping subset or in the ssp585 ensemble; MIROC6 implausibly has virtually no sea ice
243 year-round (Shu et al., 2020) and therefore zero trends (Holmes et al., 2022) leading to weaker mean trends and slightly greater
244 consistency with observations. In summary, these effects are small, and so our conclusions are robust to these sensitivity tests.

245

246 **Code Availability**

247 The code for calculating trends, performing the evaluation and preparing figures is available from the corresponding author on
248 request.

249 **Data Availability**

250 Sea Ice Area from the CMIP6 models is available from the University of Hamburg (UHH) CMIP6 Sea Ice Area directory
251 (<https://www.cen.uni-hamburg.de/en/icdc/data/cryosphere/cmip6-sea-ice-area.html>, accessed 2023-08-17). The NSIDC Sea
252 Ice Index v3.0 SIA (Fetterer, 2017) is available from <https://nsidc.org/arcticseaicenews/sea-ice-tools/>. Other observational
253 estimates of sea ice area (Dörr, 2021) are available from <https://doi.org/10.25592/uhhfdm.8559>.

254 **Author Contributions**

255 CRH, TJB and PRH conceived the study. CRH conducted the analysis and prepared the figures. All authors discussed the
256 results and reviewed the manuscript.

257 **Competing Interests**

258 The authors declare they have no conflicts of interest.

259 **Acknowledgements**

260 All authors received funding from NERC grant DEFIANT (NE/W004739/1); JS also received funding from Canada 150
261 Research Chairs program (C150 grant no. 50296). The World Climate Research Programme's (WCRP) Working Group on
262 Coupled Modelling, which is responsible for CMIP, and the climate modelling groups, are thanked for producing and making
263 available their model output.

- 265 Bracegirdle, T. J., Hyder, P., and Holmes, C. R.: CMIP5 diversity in southern westerly jet projections related to historical sea
266 ice area: Strong link to strengthening and weak link to shift, *J. Climate*, 31, 195-211, 2018.
- 267 Bracegirdle, T. J., Stephenson, D. B., Turner, J., and Phillips, T.: The importance of sea ice area biases in 21st century
268 multimodel projections of Antarctic temperature and precipitation, *Geophys. Res. Lett.*, 42, 10,832-810,839, 2015.
- 269 Diamond, R., Sime, L.C., Schroeder, D., and Holmes, C.R.: CMIP6 models rarely simulate Antarctic winter sea-ice anomalies
270 as large as observed in 2023, *Geophys. Res. Lett.*,(accepted) (2024)
- 271 Dörr, J. N., Dirk; Kern, Stefan: UHH sea-ice area product, 1850-2019 (v2019_fv0.01) [dataset],
272 <https://doi.org/10.25592/uhhfdm.8559>, , 2021.
- 273 Eyring, V., Bony, S., Meehl, G. A., Senior, C. A., Stevens, B., Stouffer, R. J., and Taylor, K. E.: Overview of the Coupled
274 Model Intercomparison Project Phase 6 (CMIP6) experimental design and organization, *Geosci. Model Dev.*, 9, 1937-1958,
275 2016.
- 276 Ferreira, D., Marshall, J., Bitz, C. M., Solomon, S., and Plumb, A.: Antarctic Ocean and sea ice response to ozone depletion:
277 A two-time-scale problem, *J. Climate*, 28, 1206-1226, 2015.
- 278 Fetterer, F., K. Knowles, W. N. Meier, M. Savoie, and A. K. Windnagel.: Sea Ice Index, Version 3 Boulder, Colorado USA.
279 National Snow and Ice Data Center. [dataset], <https://doi.org/10.7265/N5K072F8>, 2017.
- 280 Fox-Kemper, B., H.T. Hewitt, C. Xiao, G. Aðalgeirsdóttir, S.S. Drijfhout, T.L. Edwards, N.R. Golledge, M. Hemer, R.E.
281 Kopp, G. Krinner, A. Mix, D. Notz, S. Nowicki, I.S. Nurhati, L. Ruiz, J.-B. Sallée, A.B.A. Slangen Y. Yu: Ocean, Cryosphere
282 and Sea Level Change, 1211-1362, 10.1017/9781009157896.011., 2021.
- 283 Gagné, M. È., Gillett, N., and Fyfe, J.: Observed and simulated changes in Antarctic sea ice extent over the past 50 years,
284 *Geophys. Res. Lett.*, 42, 90-95, 2015.
- 285 Gupta, A. S., Jourdain, N. C., Brown, J. N., and Monselesan, D.: Climate Drift in the CMIP5 Models, *J. Climate*, 26, 8597-
286 8615, <https://doi.org/10.1175/JCLI-D-12-00521.1>, 2013.
- 287 Hawkins, E. and Sutton, R.: Time of emergence of climate signals, *Geophys. Res. Lett.*, 39, 2012.
- 288 Hobbs, W. R., Bindoff, N. L., and Raphael, M. N.: New Perspectives on Observed and Simulated Antarctic Sea Ice Extent
289 Trends Using Optimal Fingerprinting Techniques, *J. Climate*, 28, 1543-1560, <https://doi.org/10.1175/JCLI-D-14-00367.1>,
290 2015.
- 291 Holmes, C., Bracegirdle, T., and Holland, P.: Antarctic sea ice projections constrained by historical ice cover and future global
292 temperature change, *Geophys. Res. Lett.*, 49, e2021GL097413, 2022.
- 293 Holmes, C. R., Holland, P. R., and Bracegirdle, T. J.: Compensating biases and a noteworthy success in the CMIP5
294 representation of Antarctic sea ice processes, *Geophys. Res. Lett.*, 46, 4299-4307, 2019.
- 295 Kostov, Y., Marshall, J., Hausmann, U., Armour, K. C., Ferreira, D., and Holland, M. M.: Fast and slow responses of Southern
296 Ocean sea surface temperature to SAM in coupled climate models, *Clim. Dynam.*, 48, 1595-1609, 2017.
- 297 National Academies of Sciences, E. and Medicine: Antarctic sea ice variability in the southern ocean-climate system:
298 Proceedings of a workshop, 2017.
- 299 Notz, D.: Sea-ice extent and its trend provide limited metrics of model performance, *Cryosphere*, 8, 229-243, 2014.
- 300 O'Neill, B. C., Tebaldi, C., Van Vuuren, D. P., Eyring, V., Friedlingstein, P., Hurtt, G., Knutti, R., Kriegler, E., Lamarque, J.-
301 F., and Lowe, J.: The scenario model intercomparison project (ScenarioMIP) for CMIP6, *Geosci. Model Dev.*, 9, 3461-3482,
302 2016.
- 303 Parkinson, C. L.: A 40-y record reveals gradual Antarctic sea ice increases followed by decreases at rates far exceeding the
304 rates seen in the Arctic, *Proceedings of the National Academy of Sciences*, 116, 14414-14423, 2019.
- 305 Polvani, L. M. and Smith, K. L.: Can natural variability explain observed Antarctic sea ice trends? New modeling evidence
306 from CMIP5, *Geophys. Res. Lett.*, 40, 3195-3199, <https://doi.org/10.1002/grl.50578>, 2013.
- 307 Purich, A. and Doddridge, E. W.: Record low Antarctic sea ice coverage indicates a new sea ice state, *Communications Earth
308 & Environment*, 4, 314, 2023.
- 309 Roach, L. A., Dörr, J., Holmes, C. R., Massonnet, F., Blockley, E. W., Notz, D., Rackow, T., Raphael, M. N., O'Farrell, S. P.,
310 Bailey, D. A., and Bitz, C. M.: Antarctic Sea Ice Area in CMIP6, *Geophys. Res. Lett.*, 47, e2019GL086729,
311 <https://doi.org/10.1029/2019GL086729>, 2020.

312 Rosenblum, E. and Eisenman, I.: Sea ice trends in climate models only accurate in runs with biased global warming, *J. Climate*,
313 30, 6265-6278, 2017.

314 Schlosser, E., Haumann, F. A., and Raphael, M. N.: Atmospheric influences on the anomalous 2016 Antarctic sea ice decay,
315 *Cryosphere*, 12, 1103-1119, 2018.

316 Schneider, D. P. and Deser, C.: Tropically driven and externally forced patterns of Antarctic sea ice change: Reconciling
317 observed and modeled trends, *Clim. Dynam.*, 50, 4599-4618, 2018.

318 Schroeter, S., O’Kane, T. J., and Sandery, P. A.: Antarctic sea ice regime shift associated with decreasing zonal symmetry in
319 the Southern Annular Mode, *Cryosphere*, 17, 701-717, 2023.

320 Seviour, W., Codron, F., Doddridge, E. W., Ferreira, D., Gnanadesikan, A., Kelley, M., Kostov, Y., Marshall, J., Polvani, L.,
321 and Thomas, J.: The Southern Ocean sea surface temperature response to ozone depletion: A multimodel comparison, *J.*
322 *Climate*, 32, 5107-5121, 2019.

323 Shu, Q., Wang, Q., Song, Z., Qiao, F., Zhao, J., Chu, M., and Li, X.: Assessment of sea ice extent in CMIP6 with comparison
324 to observations and CMIP5, *Geophys. Res. Lett.*, 47, e2020GL087965, 2020.

325 Siegert, M. J., Bentley, M. J., Atkinson, A., Bracegirdle, T. J., Convey, P., Davies, B., Downie, R., Hogg, A. E., Holmes, C.,
326 and Hughes, K. A.: Antarctic extreme events, *Frontiers in Environmental Science*, 11, 1229283, 2023.

327 Swart, N., Martin, T., Beadling, R., Chen, J.-J., England, M. H., Farneti, R., Griffies, S. M., Hatterman, T., Haumann, F. A.,
328 and Li, Q.: The Southern Ocean Freshwater release model experiments Initiative (SOFIA): Scientific objectives and
329 experimental design, *EGUsphere*, 2023, 1-30, 2023.

330 Turner, J. and Comiso, J.: Solve Antarctica’s sea-ice puzzle, *Nature*, 547, 275-277, 2017.

331 Turner, J., Phillips, T., Marshall, G. J., Hosking, J. S., Pope, J. O., Bracegirdle, T. J., and Deb, P.: Unprecedented spring time
332 retreat of Antarctic sea ice in 2016, *Geophys. Res. Lett.*, 44, 6868-6875, 2017.

333 Zhang, L., Delworth, T. L., Cooke, W., and Yang, X.: Natural variability of Southern Ocean convection as a driver of observed
334 climate trends, *Nat. Clim. Change*, 9, 59-65, 2019.

335 Zhang, L., Delworth, T. L., Yang, X., Zeng, F., Lu, F., Morioka, Y., and Bushuk, M.: The relative role of the subsurface
336 Southern Ocean in driving negative Antarctic Sea ice extent anomalies in 2016–2021, *Communications Earth & Environment*,
337 3, 302, 2022.

338 Zunz, V., Goosse, H., and Massonnet, F.: How does internal variability influence the ability of CMIP5 models to reproduce
339 the recent trend in Southern Ocean sea ice extent?, *Cryosphere*, 7, 451-468, 2013.

340